JOURNAL OF BIOMOLECULAR STRUCTURE AND DYNAMICS
https://doi.org/10.1080/07391102.2020.1798286

Identification of potential drug candidates to combat COVID-19: a structural study using the main protease (mpro) of SARS-CoV-2

Pradeep Sharma[a†], Viswanathan Vijayan[a†], Pradeep Pant[b], Mohita Sharma[c], Naval Vikram[d], Punit Kaur[a], T. P. Singh[a] and Sujata Sharma[a]

[a]Department of Biophysics, All India Institute of Medical Sciences, New Delhi, India; [b]Computational Biochemistry, University of Duisburg, Essen, Germany; [c]Tirupati Eye and Research Centre, Noida, India; [d]Department of Medicine, All India Institute of Medical Sciences, New Delhi, India

Communicated by Ramaswamy H. Sarma

ABSTRACT

The recent outbreak of the SARS-CoV-2 virus leading to the disease COVID 19 has become a global pandemic that is spreading rapidly and has caused a global health emergency. Hence, there is an urgent need of the hour to discover effective drugs to control the pandemic caused by this virus. Under such conditions, it would be imperative to repurpose already known drugs which could be a quick and effective alternative to discovering new drugs. The main protease (Mpro) of SARS-COV-2 is an attractive drug target because of its essential role in the processing of the majority of the non-structural proteins which are translated from viral RNA. Herein, we report the high-throughput virtual screening and molecular docking studies to search for the best potential inhibitors against Mpro from FDA approved drugs available in the ZINC database as well as the natural compounds from the Specs database. Our studies have identified six potential inhibitors of Mpro enzyme, out of which four are commercially available FDA approved drugs (Cobicistat, Iopromide, Cangrelor, and Fortovase) and two are from Specs database of natural compounds (Hopeaphenol and Cyclosieversiodide-A). While Cobicistat and Fortovase are known as HIV drugs, Iopromide is a contrast agent and Cangrelor is an anti-platelet drug. Furthermore, molecular dynamic (MD) simulations using GROMACS were performed to calculate the stability of the top-ranked compounds in the active site of Mpro. After extensive computational studies, we propose that Cobicistat and Hopeaphenol show potential to be excellent drugs that can form the basis of treating COVID-19 disease.

ARTICLE HISTORY
Received 4 June 2020
Accepted 15 July 2020

KEYWORDS
COVID-19; drug repurposing; virtual screening; MD simulation; Corona virus; docking; Cobicistat

1. Introduction

A novel deadly coronavirus known as severe acute respiratory syndrome-coronavirus 2 (SARS-CoV-2) has led to a worldwide health emergency (Lai et al., 2020). The infection caused by this virus is so severe that it has already killed more than 0.2 million around the world till 02 May 2020 and infected more than 2.5 million people since its first case was reported in December 2019 in Wuhan city of China (Wang et al., 2020). World Health Organization (WHO) has named the illness caused by SARS-CoV-2 as COVID-19 and it has already been declared as pandemic on March 11, 2020 (Huang et al., 2020). This viral infection has given rise to the socio-economic emergency around the globe. At present no treatment is available for COVID-19. The main limitations of new drug discovery and development are the slow pace, high attrition rates, and expensive costs. Hence, repurposing of the known drugs to treat the diseases which need an urgent cure is gradually becoming a more practical and viable proposition because it involves the use of verified drugs with lower costs and timelines (Boopathi et al., 2020; Xue et al., 2018).

SARS-COV-2 affects the lungs causing severe respiratory syndrome in humans (Li & Xia, 2020). It is a positive-strand RNA virus having a genome size of around 30 kb which translates into 29 different proteins (Fehr & Perlman, 2015). These proteins perform various functions for virus survival from translating the genome to suppressing the host immune system. The first protein of coronavirus which is synthesized inside the human infected cell is a polyprotein consisting of a chain of 16 proteins (Hilgenfeld, 2014). The main protease, also called Mpro or 3CLpro acts as molecular scissor which cuts these proteins into individual units to function independently. This protease is essential for virus survival because its function is responsible for the processing of all the non-structural proteins translated from viral RNA. Hence this is an excellent drug target amongst all the proteins of the coronavirus (Anand et al., 2003).

The three-dimensional crystal structure of the main protease from SARS-CoV-2 has recently been deposited in the protein data bank (PDB ID: 6Y2F). This structure can be used to identify potential inhibitors using virtual screening and docking studies. Structurally, Mpro from both SARS-COV and SARS-COV-2 is very similar. The molecule consists of an

CONTACT Sujata Sharma sujatasharma.aiims@gmail.com Department of Biophysics, All India Institute of Medical sciences, New Delhi 110029, India.
†Authors contributed equally.

antiparallel beta barrel divided into two domains with an alpha helical region forming the third domain. The substrate binding site is situated between the two beta-barrel domains. The alpha-helical domain is responsible for the dimerization of the Mpro which is essential for the function of the enzyme. The N-finger (the first seven N-terminal residues) of one monomer interacts with the Glu166 of the other monomer, thereby shaping the S1 subsite of the substrate-binding site (Yang et al., 2003). Previous reports have shown that residues 41, 140, 142-145, 161, 163, 166, and 172 form the major part of the active site. Additionally, the conserved residues, His41, and Cys145 play an important role in the catalysis (Zhang et al., 2020). The importance of these residues has been shown by mutational studies as mutating these two residues leads to a loss of protease activity (Huang et al., 2004). Drug repurposing has been extensively done against many protein targets of this virus, the Main protease has been targeted for natural compounds, antivirals, plant alkaloids, phytochemicals, many other drugs like alcoholism averting drug, Disulfiram but no compound has been effective till date (Aanouz et al., 2020; Adeoye et al., 2020; Al-Khafaji et al., 2020; Elmezayen et al., 2020; Gyebi et al., 2020; Islam et al., 2020; Joshi et al., 2020; Khan, Jha, et al., 2020; Khan, Zia, et al., 2020; Lobo-Galo et al., 2020; Muralidharan et al., 2020). Spike protein and ACE2 complex has been targeted for drug repurposing, many natural products, stilbenoid analogs have been docked and their binding affinities have been calculated (Elfiky, 2020; Gupta et al., 2020; Hasan et al., 2020; Sinha et al., 2020; Wahedi et al., 2020; Kumar et al., 2020; Pant et al., 2020). Sarma et al have identified theophylline and pyrimidone derivatives as inhibitors against RNA binding to the N terminal domain of N protein of coronavirus (Sarma et al., 2020). Sofosbuvir, Ribavirin, Galidesivir, Remdesivir, Favipiravir, Cefuroxime, Tenofovir, and Hydroxychloroquine have been identified as inhibitors of RNA dependent RNA polymerase (Elfiky, 2020). In this study, we have targeted the active site of the main protease of SARS-CoV-2 and virtually screened the drugs which are already FDA approved from the ZINC database and spec database of approved natural drugs from medicinal plants.

2. Material and methods

2.1. Protein and ligand preparation

The main protease of SARS-CoV-2 (Zhang et al., 2020) was selected as a target receptor protein. The coordinates of this protein were retrieved from the protein data bank (PDB ID: 6Y2F). The protein structure was imported to the Maestro v11(Schrödinger, 2017) and the structure was prepared using the protein preparation wizard of the Schrödinger-2017at physiological pH of 7.4 (Sastry et al., 2013). The protein was prepared for molecular docking by removing the ligand from its active site. Also, the missing loop residue insertion was allowed if found and the water oxygen atoms were removed and the hydrogen atoms were added. The protein was optimized and energy minimized for optimized potentials using the liquid simulations (OPLS-3) force field for all atoms in the structure (Harder et al., 2016). The dimensions of the receptor grid-box generated using Glide v7.1 (Friesner et al., 2006) were 5 Å × 5 Å × 5 Å around the center of the active site residues of the protein to ensure that all the extended conformations of ligand fits within the grid box. The ligands were retrieved from the ZINC database (FDA drug) (Sterling & Irwin, 2015) and Spec database (Natural compound from medicinal plants) in SDF file formats. The downloaded ligands were prepared for docking using the Ligprep module (Schrödinger, 2017). Ligands were minimized using the OPLS-3 force field. All the compounds were energy minimized by the addition of hydrogen atoms. Finally, these compounds were converted to low energy structures with correct chirality, ionization states, tautomeric states, stereochemistries, and ring conformation (Schrödinger, 2017).

2.2. Screening the compounds

High Throughput Virtual screening (HTVs) was performed by the Glide docking module (Friesner et al., 2006) using a grid receptor with the set of ligands. A total of 2100 FDA approved drugs from the ZINC database and 400 compounds from the Spec database were used for HTV. After screening all the compounds against the receptor grid box using the HTVs docking module, fifty compounds from the FDA approved drugs and twenty compounds from medicinal plants were selected based on their docking score, glide energy and hydrogen bond interactions. The selected ligands were subjected to Extra Precision (XP)glide docking in which the constructed grid on the receptor was held rigid while docking. The XP glide scoring of docked ligand was carried out based on the docking score and energy. Four from FDA approved drugs and two ligands from medicinal plants were selected to proceed with induced fit docking.

2.3. Induced fit docking

Induced fit docking (IFD) was carried out for six ligands using the molecular modeling software GLIDE of Maestro v11, Schrodinger suite 2017 (Friesner et al., 2006). The energy minimized COVID-19 receptor active site residues were used to generate the grid box which was subjected to the IFD studies. The energetically favourable docked poses were obtained for all 6 ligands and the best poses were chosen based on the glide energy, docking score, hydrogen bond, and hydrophobic interactions.

2.4. Molecular dynamic simulation

The stability of the interactions of the drug molecules (both FDA approved drugs and natural compounds) with SARS-CoV2-Mpro is essential to understand its binding affinity with the drug target. The top binding poses of drug-like molecules with SARS-CoV2-Mpro from the molecular docking results were subjected to MD simulation using GROMACS package version 5.0.6 (Kutzner et al., 2007). The topology of SARS-CoV2-Mpro protein was generated by the GROMOS96 54a7 force field. The topology of ligands was generated from the PRODRG online server and used for the initial protein-

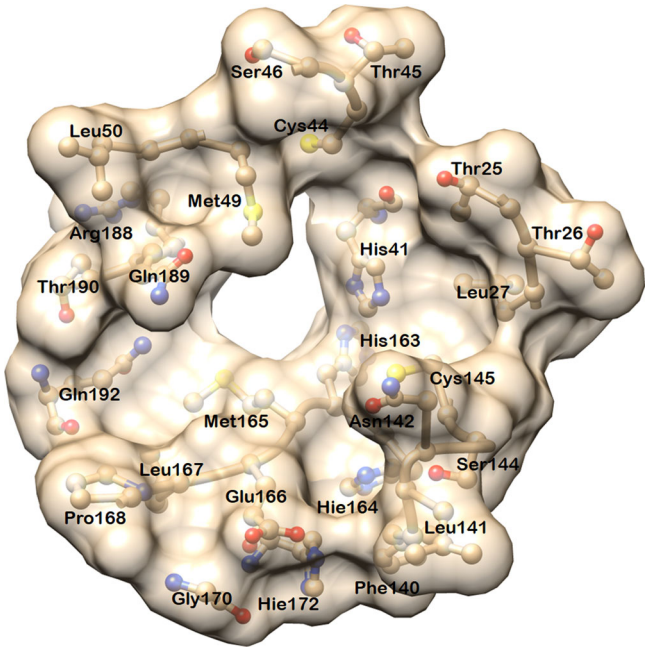

Figure 1. Diagram showing the active site residues of the main protease (Mpro) of SARS-CoV-2. The area and volume of the binding site are 335.94 Å^2 and 364.1 Å^3 respectively. This site was used for screening and docking the compounds from drug databases.

ligand molecular dynamic simulation runs. The protein molecule kept at the center of the cubic cell and the periodic boundary condition was 1 Å from all the directions. The cell was solvated by an explicit SPC water model and the system was neutralized by adding appropriated counter ions. To minimize the energy, the system was allowed to converge at the tolerance of 1000 kJ mol^{-1} nm^{-1} with 500 steps of steepest descent. Similarly, the conjugate gradient method was run with the same parameter set up for further minimization of the system. During the MD process, the LINCS algorithm (Hess et al., 1997) was employed for all covalent bonds in protein and long-range electrostatic interactions were computed using Partial Mesh Ewald method (Kawata & Nagashima, 2001) (PME). The geometry of water molecules was constrained by SETTLE algorithm (Miyamoto & Kollman, 1992). To equilibrate the system, v-rescale temperature (Berendsen et al., 1984) scaling method was implemented for NVT equilibration at 330 K and then, Parrinello–Rahman (Parrinello & Rahman, 1981) pressure coupling method was executed for NPT equilibration at 1 bar pressure. The time of both equilibrations was 500 ps. The MD simulation was performed to 100 ns time steps for all the molecules. The output energy and coordinate were stored in the trajectory for every 2 ps and they were analyzed using the Gromacs analysis tool (Xmgrace).

2.5. Binding free energy calculation

The molecular dynamic trajectory was used for calculation of the binding free energy (ΔG_{bin}) between protein and ligands. The binding free energy depends on three factors; the gas-phase free energy (ΔGMM), the solvation free energy (ΔGsol) and the change in the system entropy ($-T\Delta S$), which can be calculated by molecular mechanics Poisson-Boltzmann Surface Area (MM-PBSA) module, as expressed in Equation (1) (Kollman et al., 2000):

$$\Delta G\text{bin} = \Delta G\text{MM} + \Delta G\text{sol} - T\Delta S \quad (1)$$

In this study, MM-PBSA calculations were performed using GMXPBSA 2.1: A GROMACS tool to calculate the interaction energy between the ligand and the residues of the protein active site as discussed in the ligand-protein interaction section.

2.6. Electrostatic potential calculation

The respective output files of the structures were saved in the pqr file format that contains the information about the partial charge and radius of each atom. The electrostatic surface potential of the complexes with the best free energy values was generated and viewed using PyMol software (DeLano, 2002).

3. Result and discussion

3.1. Docking

The docked complexes of six ligands (four from the FDA drug and two from medicinal plant compound databases) with Mpro show that these ligands are positioned in the active site with the active participation of hydrogen bonds and hydrophobic contacts with the residues of Mpro. In the crystal structure (PDB ID: 6Y2F), the active site cavity is a well-defined pocket with the area and volume of 335.94 Å^2 and 364.1 Å^3, respectively (Figure 1).

This paves a way for binding of inhibitors like alpha-ketoamide (O6K) which has ligand interface area and volume of 634.2 Å^{2}and 570.1 Å^3, respectively. In comparison with the co-crystal inhibitor, the selected docked molecules have shown the ligand interface area and volume of 540.0 Å^2 and 640.7 Å^3 for Fortovase (ZINC-26664090), 607.2 Å^2 and 752.1 Å^3 for Cobicistat (ZINC-85537014), 533.8 Å^2 and 567.7 Å^3 for Cangrelor (ZINC-85537017), 452.9 Å^2 and 576.8 Å^3 for Iopromide (ZINC-3830958), 621.6 Å^2 and 791.2 Å^3 for Hopeaphenol (AA-504/21113022) and 598.7 Å^2 and 780.7 Å^3 for Cyclosieversiodide-A (AH-214/21172036) respectively.

All the compounds occupied the active site in a varied manner. The co-crystal ligand Alpha-ketoamide was docked at the active site residues of Mpro of SARS-CoV-2 and the docking score and glide energy was calculated as −10.983 and −78.884 kcal/mol, respectively. Alpha-ketoamide formed hydrogen bond interactions with the residues Asn142, Gly143, Glu166, Gln189, and Gln192 (Figure 2) and also formed several hydrophobic contacts with neighbouring residues.

Cobicistat, an HIV drug that showed the docking score and glide energy of −12.318 and −93.052 kcal/mol respectively. This 5 ringed drug formed 6 hydrogen bond interactions with the His41, Cys145, Glu166, Gln189, and Thr190 (Figure 3).

This drug formed strong hydrogen bonds with both the catalytic residues, Cys145 and His41, as well as other residues

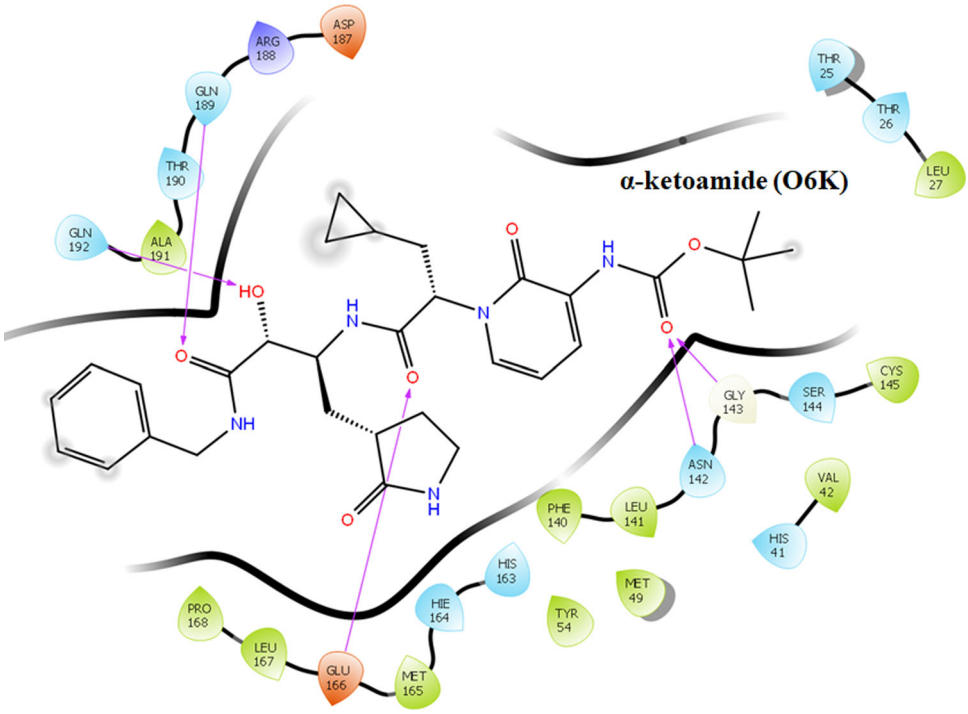

Figure 2. Ligand interaction diagram showing the interactions of the co-crystallized ligand α-ketoamide (O6K) and active site residues of Mpro.

of the substrate-binding site. Cangrelor, an antiplatelet drug is a nucleoside triphosphate analogue that is oriented towards the distal part of the cavity and forms strong hydrogen bond interactions with the residues of Phe140, Gly143, Glu166, and Gln189 (Figure 4A). The docking score and glide energy of Cangrelor are −12.284 and −88.723 kcal/mol, respectively.

The next drug Fortovase used widely for controlling HIV formed 7 hydrogen bond interactions with the Phe140, Gly143, Ser144, Glu166, and Gln189 but did not form any hydrogen bonds with the catalytic residues, Cys145 and His41 (Figure 4B). It showed a docking score and glide energy of −10.284 and −81.886 kcal/mol, respectively.

The Iopromide interacts with active site residues by forming 9 hydrogen bond interactions with Asn142, Hie164, Glu166, Arg188, Gln189, Thr190, and Gln192 and displayed a docking score and glide energy of −14.261 and −95.137 kcal/mol, respectively (Figure 4C).

Hopeaphenol, a resveratrol tetramer forms hydrogen bond interactions with residues Ser46, Glu47, Met49, Asn142, Gly143, Hie164, Glu166, Gln189, Thr190 and Gln192 of Mpro and the docking score and glide energy of this complex are −14.273 and −99.273 kcal/mol, respectively (Figure 3A & C).

Cyclosieversiodide-A, the other compound from medicinal plants interacted with the residues Phe140, Asn142, Ser144, Glu166, Gln189, and Gln192, and also the active site residue His41 and showed a docking score and glide energy of −11.263 and −94.126 kcal/mol, respectively (Figure 4D). All the results of docking are summarized in Table 1.

3.2. Molecular dynamic simulation

The alpha-ketoamide inhibitor complex of SARS-CoV2-Mpro was considered as a reference drug molecule throughout the MD simulation analysis. The native form of Mpro was also included to check the overall conformational changes in the protein molecule when these drug molecules interact with the protein. The MD results suggested that the interaction of Cobicistat and Iopromide molecules with SARS-CoV2-Mpro leads to a reduction in the Root Mean square Deviation (RMSD) values when compared with the native and Alpha-ketoamide bound SARS-CoV2-Mpro. When the RMSD profiles of the complexes of Cobicistat and Iopromide were compared, we found the values less in case of Cobicistat than Iopromide complex that shows the Cobicistat complex is more stable (Figure 5A). Though both the drugs Cobicistat and Iopromide showed a good RMSD profile, it is suggested that Cobicistat would have a better binding pattern with SARS-CoV2-Mpro than Iopromide. The root mean square fluctuation (RMSF) values showed that Cobicistat interacts with more residues of the active site than Iopromide and Alpha-ketoamide (Figure 5B). Cobicistat also interacts with both the main catalytic residues of this protease, His41, and Cys145. All the fluctuations of the active site residues were impeded by cobicistat throughout the MD run. The radius of gyration (Rg) of all the complexes ranged from 2.15 to 2.30 nm. These values indicate that there was not much change in the overall globular structure of the protein after the binding of these ligands (Figure 5C). This analysis showed that the Cobicistat had better and stable interaction with SARS-CoV2-Mpro than the reference drug molecule Alpha-ketoamide. Moreover, this data also indicated that Iopromide can also be the potential inhibitor of this protease along with Cobicistat.

On the other hand, similar MD analysis was performed with best-docked poses of natural compounds with SARS-CoV2-Mpro, with alpha-ketoamide as a reference drug for comparison. The RMSD graph indicated that the value of RMSD was below 3 Å (avg RMSD ~2 Å) in case of the

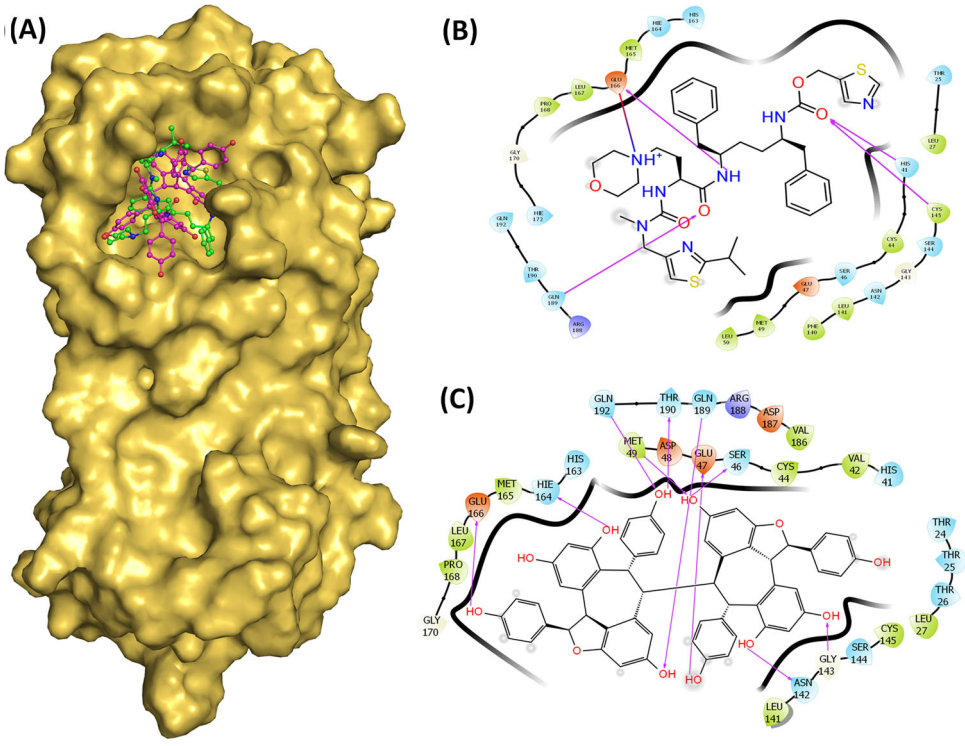

Figure 3. (A) Surface diagram showing the position of Cobicistat and Hopeaphenol in the active site. (B) Ligand interaction diagram showing hydrogen and hydrophobic interactions of Cobicistat with Mpro. (C) Ligand interaction diagram showing hydrogen and hydrophobic interactions of Hopeaphenol with Mpro.

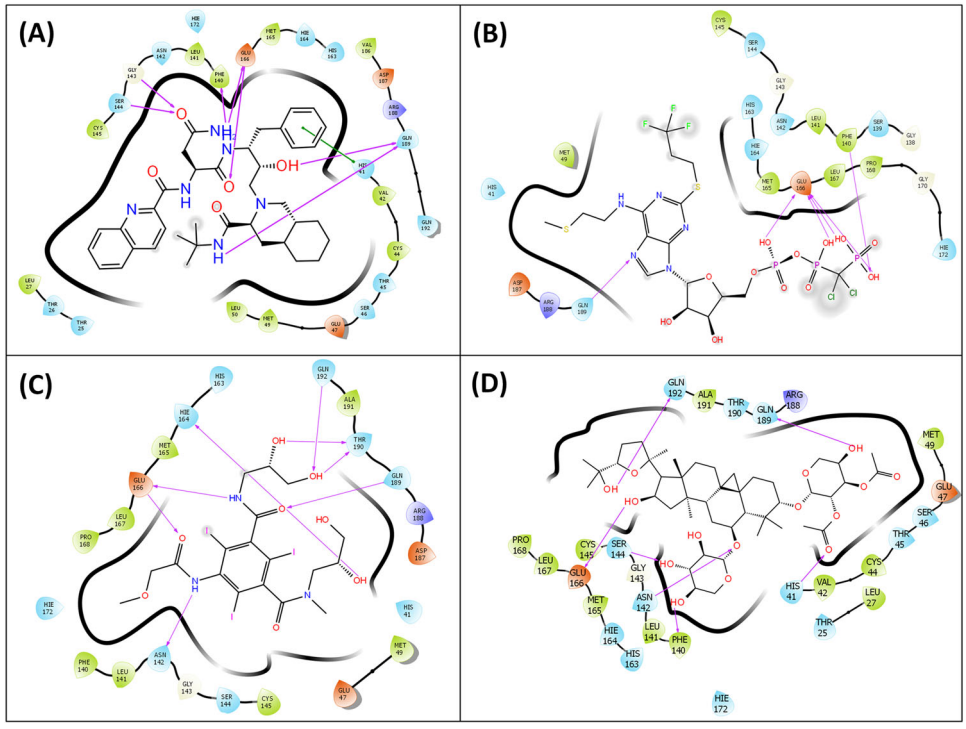

Figure 4. (A) Ligand interaction diagram showing hydrogen and hydrophobic interactions of Cangrelor with Mpro. (B) Ligand interaction diagram showing hydrogen and hydrophobic interactions of Fortovase with Mpro. (C) Ligand interaction diagram showing hydrogen and hydrophobic interactions of Iopromide with Mpro. (D) Ligand interaction diagram showing hydrogen and hydrophobic interactions of Cyclosieversiodide-A with Mpro.

Hopeaphenol and it was more than 4 Å in case of the reference drug. This result indicates that Hopeaphenol complex is more stable (Figure 6A). The results of Root Mean Square Fluctuation (RMSF) indicated that the natural compound Hopeaphenol impedes the fluctuations of the residues throughout the MD run (Figure 6B). The radius of gyration of SARS-CoV2-Mpro in native and ligand-bound forms varied between 2.10 to 2.30 nm (Figure 6C). This result showed that there was not any significant change in the overall globular structure of the protein.

These results indicate that the natural compound Hopeaphenol could be a potential molecules which can

Table 1. Docking score and glide energy (in kcal/mol) of co-crystal (Alpha-ketoamide) inhibitor, FDA approved drugs and medicinal plant compounds with main protease (MPro) of SARS-CoV-2 (PDB ID: 6Y2F).

Compounds	Hydrogen binding interactions	Distance (Å)	Hydrophobic interactions	Docking Score (kcal/mol)	Glide Energy (kcal/mol)
	Asn142(N—H … O)	3.23			
Co-crystal (O6K)	Gly143(N—H … O)	2.77	Thr25, Thr26, Leu27, His41, Val42, Met49, Tyr54, Phe140, Leu141, Ser144, Cys145, His163, Hie164, Met165, Leu167, Pro168, Asp187, Arg188, Thr190 and Ala191	−10.983	−78.884
Alpha-ketoamide	Glu166(N—H … O)	2.72			
	Glu166(N—H … O)	2.95			
	Gln189(N—H … O)	2.87			
	Gln192(N—H … O)	3.18			
	Phe140 (N—H … O)	2.77			
ZINC-26664090	Gly143(O—H … O)	3.02	Thr25, Thr26, Leu27, His41, Val42, Cys44, Thr45, Ser46, Glu47, Met49, Leu50, Leu141, Asn142, Cyc145, His163, Hie164, Met165, Hie172, Val186, Asp187, Arg188 and Gln192	−10.283	−81.886
(Fortovase)	Ser144(O—H … O)	3.26			
	Glu166(N—H … O)	3.08			
	Glu166 (N—H … O)	3.01			
	Gln189 (O—H … O)	3.14			
	Gln189 (N—H … O)	2.84			
	His41(N—H … O)	3.05			
ZINC-85537014	Cys145(S—H … O)	2.95	Thr25, Leu27, Cys44, Thr45, Ser46, Glu47, Met49, Leu50, Phe140, Leu141, Asn142, Gly143, Ser144, His163, Hie164, Met165, Leu167, Pro168, Gly170, Hie172 and Gln192	−12.318	−93.052
(Cobicistat)	Glu166 (N—H … O)	3.00			
	Gln189(O—H … O)	3.23			
	Thr190 (N—H … O)	3.28			
	Thr190 (O—H … O)	3.06			
	Phe140(O—H … O)	3.05			
ZINC-85537017	Gly143(N—H … F)	2.91	His41, Met49, Gly138, Ser139, Leu141, Asn142, Ser144, Cys145, His163, Hie164, Met165, Leu167, Pro168, Gly170, Hie172, Asp187, Arg188 and Gln189	−12.284	−88.723
(Cangrelor)	Glu166 (O—H … O)	2.71			
	Glu166 (N—H … O)	2.84			
	Glu166 (N—H … O)	2.86			
	Glu166 (N—H … O)	2.98			
	Gln189(O—H … O)	3.28			
	Asn142(O—H … N)	2.81			
	Hie164(O—H … N)	3.11	His41, Glu47, Met49, Phe140, Leu141, Gly143, Ser144, Cys145, His163, Met165, Leu167, Pro168, Hie172, Asp187 and Ala191		
ZINC-3830958	Glu166(N—H … O)	2.79		−14.261	−95.137
(Iopromide)	Glu166 (N—H … O)	3.31			
	Arg188(O—H … N)	3.01			
	Gln189(N—H … O)	3.14			
	Thr190 (O—H … O)	2.76			
	Thr190 (O—H … O)	2.90			
	Gln192(O—H … O)	2.93			
	Ser46 (O—H … O)	2.62			
	Glu47 (O—H … O)	2.88			
AA-504/21113022 (Hopeaphenol)	Met49(N—H … O)	3.12	Thr24, Thr25, Thr26, Leu27, His41, Val42, Cys44, Asp48, Leu141, Ser144, Cys145, His163, Met165, Leu167, Pro168, Gly170, Val186, Asp187 and Arg188	−14.473	−99.413
	Asn142 (O—H … O)	2.63			
	Gly143(O—H … O)	2.97			
	Hie164 (O—H … O)	2.71			
	Glu166 (O—H … O)	3.18			
	Gln189(O—H … O)	3.08			
	Thr190 (O—H … O)	3.27			
	Gln192(O—H … O)	2.99			
	His41(O—H … O)	2.89			
	His41(O—H … N)	2.72	Thr25, Leu27, Val42, Cys44, Thr45, Ser46, Glu47, Met49, Leu141, Gly143, Cys145, His163, Hie164, Met165, Leu167, Pro168, Hie172, Arg188, Thr190 and Ala191		

(*continued*)

Table 1. Continued.

Compounds	Hydrogen binding interactions	Distance (Å)	Hydrophobic interactions	Docking Score (kcal/mol)	Glide Energy (kcal/mol)
AH-214/21172036 (Cyclosieversiodide A)	Phe140 (O—H … O)	2.76		−11.263	−94.126
	Asn142(O—H … O)	2.92			
	Ser144(O—H … O)	2.87			
	Glu166 (O—H … O)	2.95			
	Gln189 (O—H … O)	2.82			
	Gln192 (O—H … O)	3.35			

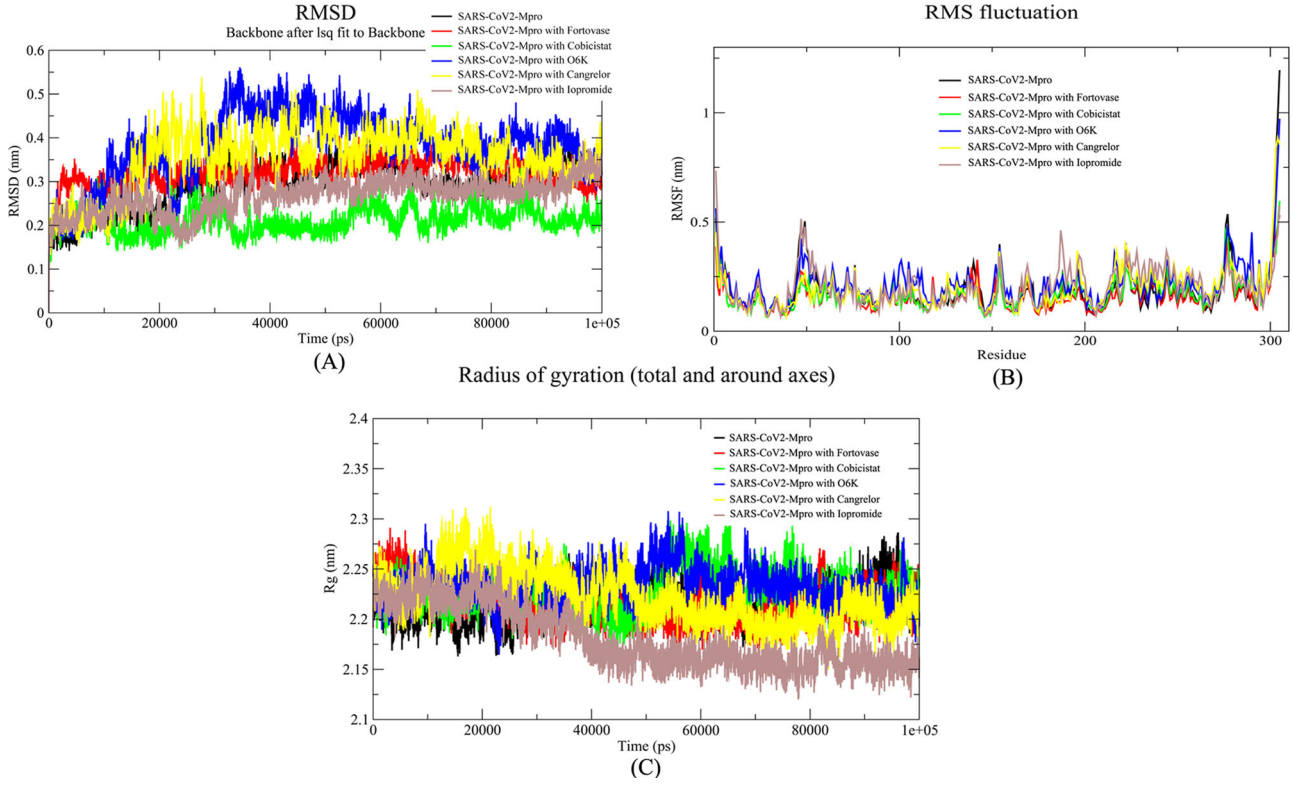

Figure 5. Analysis of the molecular dynamic simulation results of MPro, MPro-Fortovase complex, MPro-Cobicistat complex, Mpro-Cangrelor complex, MPro-Iopromide complex and MPro-α-ketoamide complex. (A) Root Mean Square Deviation (RMSD), (B) Root Mean Square fluctuation (RMSF), (C) Radius of Gyration (Rg).

inhibit the main protease of the SARS-CoV2. All the results obtained from MD simulation of these ligands are summarized in Table 2.

3.3. Binding free energy calculation

The binding free energy (MM-PBSA) was calculated after each complex reaches equilibrium during MD simulation calculations. The last 10 ns were used for calculating the binding energy of each complex and results are detailed in Table 3. Cobicistat showed the lowest binding free energy with the main protease (Mpro) among the FDA approved compounds that were identified from the ZINC database based on docking score, glide energy, and MD calculations. While Hopeaphenol depicted the lowest binding free energy among the natural compounds from the Specs database.

The number of hydrogen bonds as a function of run-length was plotted for all the systems considered for the study. The default values of hydrogen bond distance (3.5 Å) and angle (120°) was implemented for calculations. Cangrelor, Fortovase, Iopromide, cyclosieversiodide A, and native-alpha-ketoamide showed two hydrogen bonds in the active site of the protein (average value). Hopeaphenol, however, showed 3 hydrogen bonds, while cobicistat showed 4 hydrogen bonds with the protein throughout the simulations (Figure 7).

No cytochrome P450 enzymes inhibition was predicted using SwissADME webtool (http://www.swissadme.ch/index.php#), suggesting no cytotoxicity involved with these molecules. The off-target predictions were performed by utilizing a freely accessible MolTarPred webserver (http://moltarpred.marseille.inserm.fr/). This protocol uses the knowledge-driven from 607,659 compounds and 4,553 proteins collected from the ChEMBL repository. Cobicistat, cyclosieversiodide A, hopeaphenol, and native-alpha-ketoamide showed no prominent off-targets (even at a low confidence level of 70%). On the other hand, cangrelor (off-target: Purinergic receptor P2Y12), fortsovase (off-targets: Human immunodeficiency virus type 1 protease, Prelamin-A/C, Thromboxane-A synthase, Vasopressin V1a receptor), and lopromide (off-target: Prelamin-A/C) showed some off-targets with high confidence.

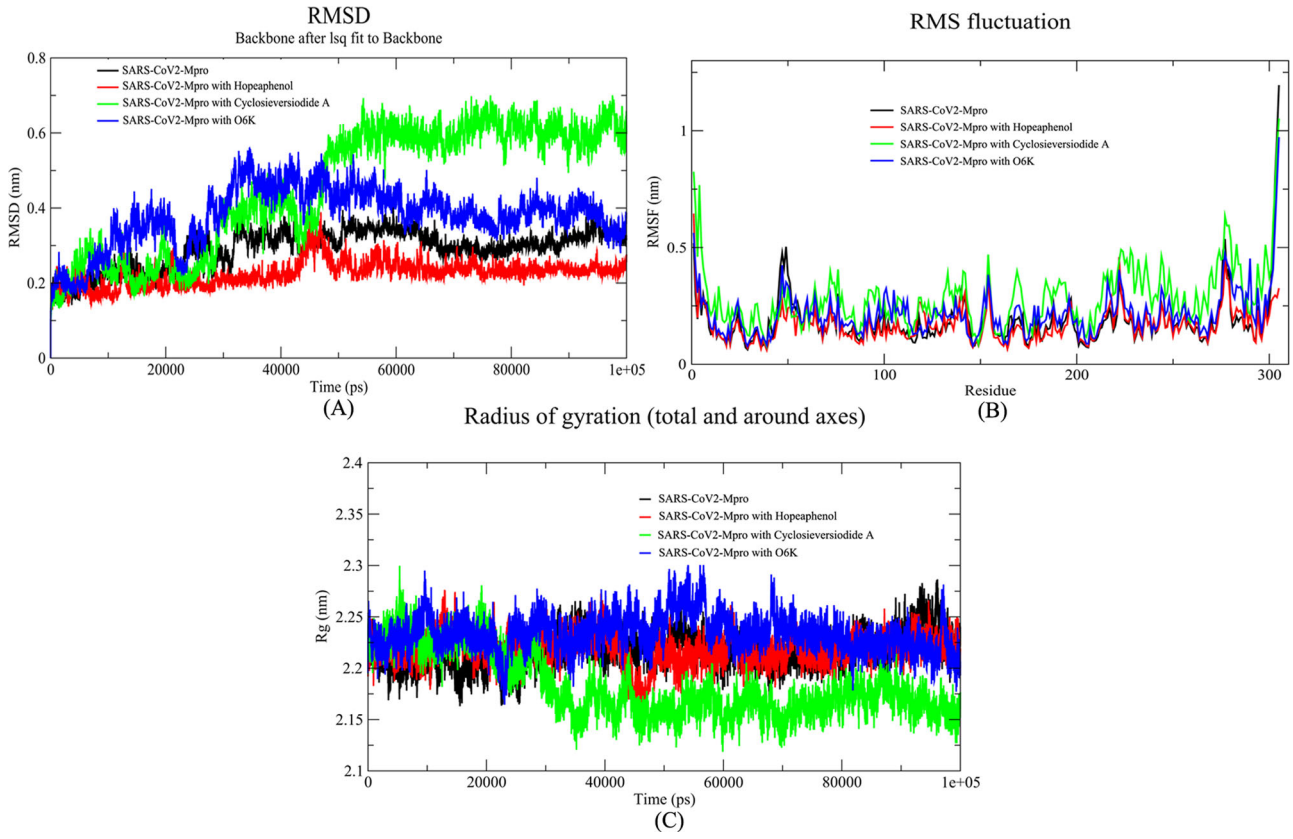

Figure 6. Analysis of the molecular dynamic simulation results of MPro, MPro-Hopeaphenol complex, MPro-Cyclosieversiodide-A complex, and MPro-α-ketoamide complex. (A) Root Mean Square Deviation (RMSD), (B) Root Mean Square fluctuation (RMSF), (C) Radius of Gyration (Rg).

Table 2. Time averaged properties calculations obtained from MD simulation of Mpro with various docked ligands.

Analysis	MPro	O6K	Fortovase	Cobicistat	Cangrelor	Iopromide	Hopeaphenol	Cyclosieversiodide A
Average RMSD (Å)	3.05	4.30	3.10	2.25	3.85	2.95	2.20	4.90
Average Rg (Å)	22.3	22.4	22.0	22.5	22.5	21.7	23.5	21.7

Table 3. Binding free energy calculations obtained after MD simulation of Mpro with various docked ligands.

Analysis	Fortovase	Cobicistat	Cangrelor	Iopromide	Hopeaphenol	Cyclosieversiodide A
Binding Free Energy (kcal/mol	−7.52	−11.42	−6.93	−8.22	−10.95	−8.54

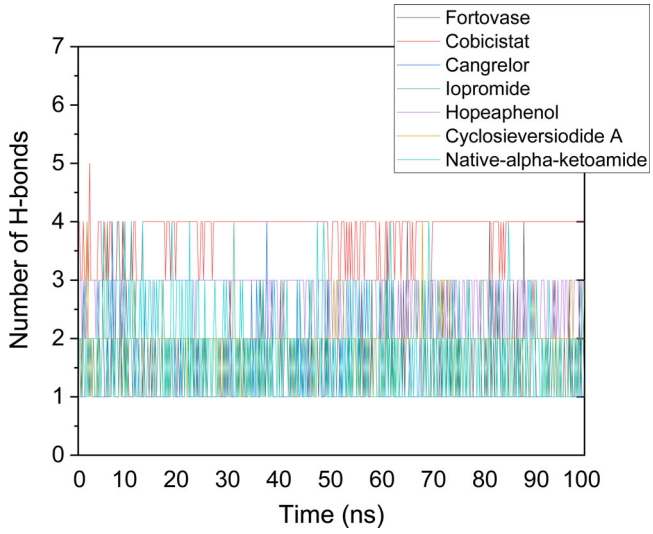

Figure 7. Plot showing the number of hydrogen bonds as the function of run length for all the ligands. Cobicistat and Hopeaphenol has shown the maximum number of hydrogen bonds throughout the simulation process.

3.4. Electrostatic potential calculation

Electrostatic potential calculations help in understanding the distribution of the charge on the protein surface and its interaction with the ligands. The cavity of the protein was negatively charged or neutral amino acids were present and the rest of the active site was positively charged (Figure 8).

4. Conclusions

COVID-19 pandemic has forced the entire scientific fraternity around the world to find some fast and effective solution against this disease. Searching a drug from scratch will be impractical at this time because of the time a drug takes for its development. Therefore, it is worthwhile to look for other drugs that have already been declared safe in humans to fight against this virus. In this study, after exhaustive computational analysis, we have identified four FDA approved drugs (Cobicistat, Iopromide, Cangrelor, and Fortovase) and two approved drugs from medicinal plants (Hopeaphenol

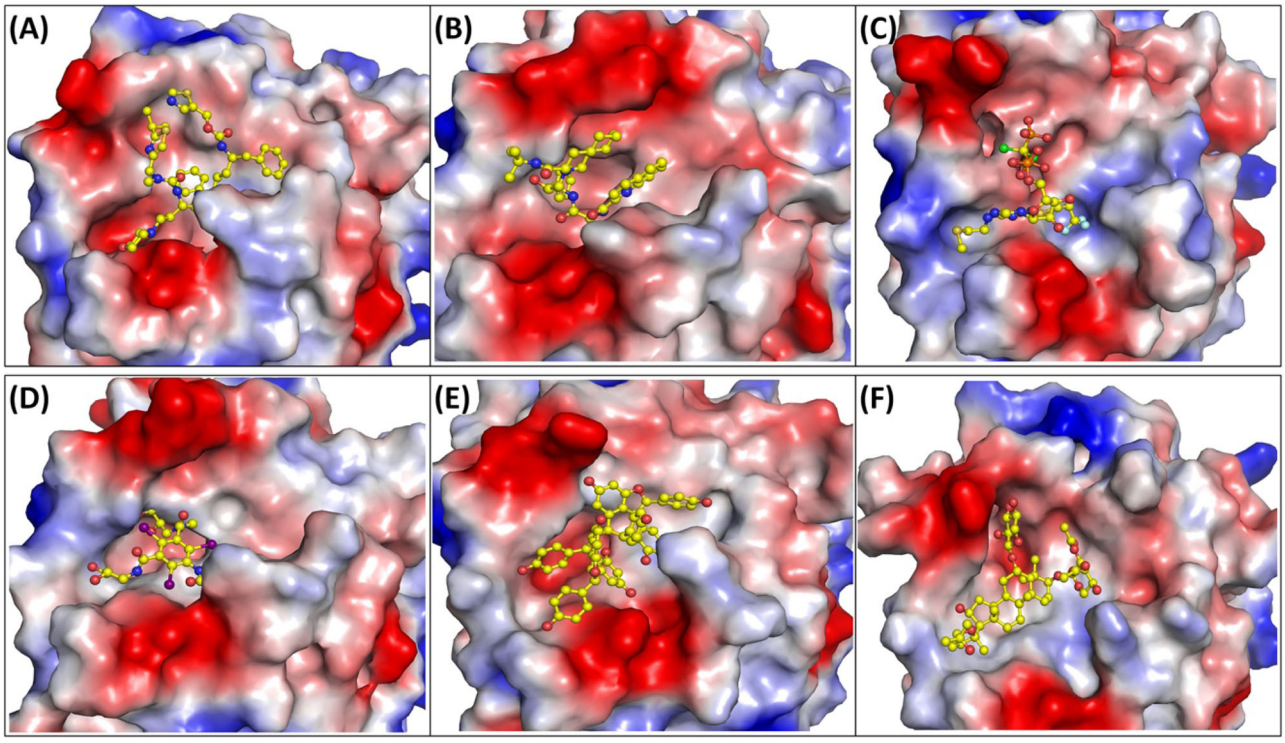

Figure 8. Electrostatic surface potential of the top ranked compounds. The electrostatic potential showing (A) Mpro and Cobicistat (B) Mpro and Fortovase (C) Mpro and Cangrelor (D) Mpro and Iopromide (E) Mpro and Hopeaphenol (F) Mpro and Cyclosieversiodide-A. Positive and negative electrostatic charges are coloured in blue and red respectively.

and Cyclosieversiodide-A) which could be potential inhibitors of the main protease of SARS-CoV-2. When the interactions of these ligands with the other homologous proteins from SARS-CoV and MERS were compared, we found that most of the residues (His41, Cys145, Glu166, Gln189 and Gln192) interacting with all the ligands are identical in SARS-CoV-2, SARS-CoV, and MERS. Some residues (Asn142 and Thr190) which were not identical were found to be similar in all the counterparts. The stability of these complexes with Mpro was checked by molecular dynamic simulation. After analyzing the MD results, found that Cobicistat and Hopeaphenol could be the potential inhibitors of the main protease that can be studied in the experimental setup. These findings would certainly help in developing the therapeutic molecules against this virus.

Acknowledgements

Dr. Pradeep Sharma and Dr. Sujata Sharma thank All India Institute of Medical sciences (AIIMS), New Delhi for intramural grant. Dr. Viswanathan V thanks Department of Science and Technology (DST), SERB for National Postdoctoral Fellowship. Dr T. P. Singh thanks Department of Science and Technology (DST) for SERB Distinguished Research Professorship.

Disclosure statement

No potential conflict of interest was reported by the authors.

Ethical standards

Ethical standards are compulsory for studies relating to human and animal subjects.

Funding

This work was supported by All-India Institute of Medical Sciences.

ORCID

Pradeep Pant http://orcid.org/0000-0003-3890-1958
Punit Kaur http://orcid.org/0000-0002-7358-3716

References

Aanouz, I., Belhassan, A., El-Khatabi, K., Lakhlifi, T., El-Ldrissi, M., & Bouachrine, M. (2020). Moroccan Medicinal plants as inhibitors against SARS-CoV-2 main protease: Computational investigations. *Journal of Biomolecular Structure and Dynamics*. https://doi.org/10.1080/07391102.2020.1758790

Adeoye, A. O., Oso, B. J., Olaoye, I. F., Tijjani, H., & Adebayo, A. I. (2020). Repurposing of chloroquine and some clinically approved antiviral drugs as effective therapeutics to prevent cellular entry and replication of coronavirus. *Journal of Biomolecular Structure and Dynamics*. https://doi.org/10.1080/07391102.2020.1765876

Al-Khafaji, K., Al-Duhaidahawil, D., & Tok, T. T. (2020). Using integrated computational approaches to identify safe and rapid treatment for SARS -CoV- 2. *Journal of Biomolecular Structure and Dynamics*. https://doi.org/10.1080/07391102.2020.1764392

Anand, K., Ziebuhr, J., Wadhwani, P., Mesters, J. R., & Hilgenfeld, R. (2003). Coronavirus main proteinase (3CLpro) structure: Basis for

design of anti-SARS drugs. *Science (New York, N.Y.).)*, *300*(5626), 1763–1767. https://doi.org/10.1126/science.1085658

Berendsen, H. J., Postma, C., Van Gunsteren, J. P. M., DiNola, W. F., & Haak, J. R. (1984). Molecular dynamics with coupling to an external bath. *Journal of* Chemical Physics., *81*(8), 3684–3690. https://doi.org/10.1063/1.448118

Boopathi, S., Poma, A. B., & Kolandaivel, P. (2020). Novel 2019 coronavirus structure, mechanism of action, antiviral drug promises and rule out against its treatment. *Journal of Biomolecular Structure and Dynamics*. https://doi.org/10.1080/07391102.2020.1758788

DeLano, W. L. (2002). Pymol: An open-source molecular graphics tool. *CCP4 Newsletter on Protein Crystallography*, *40*, 82–92.

Elfiky, A. A. (2020). Natural products may interfere with SARS-CoV-2 attachment to the host cell. *Journal of Biomolecular Structure and Dynamics*. https://doi.org/10.1080/07391102.2020.1761881

Elfiky, A. A. (2020). SARS-CoV-2 RNA dependent RNA polymerase (RdRp) targeting: An *in silico* perspective. *Journal of Biomolecular Structure and Dynamics*. https://doi.org/10.1080/07391102.2020.1761882

Elmezayen, A. D., Al-Obaidi, A., Şahin, A. T., & Yelekçi, A. (2020). Drug repurposing for coronavirus (COVID-19): *In silico* screening of known drugs against coronavirus 3CL hydrolase and protease enzymes. *Journal of Biomolecular Structure and Dynamics*. https://doi.org/10.1080/07391102.2020.1758791

Fehr, A. R., & Perlman, S. (2015). Coronaviruses: An overview of their replication and pathogenesis. *Methods in Molecular Biology (Clifton, N.J.).)*, *1282*, 1–23. https://doi.org/10.1007/978-1-4939-2438-7_1

Friesner, R. A., Murphy, R. B., Repasky, M. P., Frye, L. L., Greenwood, J. R., Halgren, T. A., Sanschagrin, P. C., & Mainz, D. T. (2006). Extra precision glide: Docking and scoring incorporating a model of hydrophobic enclosure for protein-ligand complexes. *Journal of Medicinal Chemistry*, *49*(21), 6177–6196. https://doi.org/10.1021/jm051256o

Gupta, M. K., Vemula, S., Donde, R., Gouda, G., Behera, L., & Vadde, R. (2020). *In-silico* approaches to detect inhibitors of the human severe acute respiratory syndrome coronavirus envelope protein ion channel. *Journal of Biomolecular Structure and Dynamics*. https://doi.org/10.1080/07391102.2020.1751300

Gyebi, G. A., Ogunro, O. B., Adegunloye, A. P., Ogunyemi, O. M., & Afolabi, S. O. (2020). Potential inhibitors of coronavirus 3-chymotrypsin-like protease ($3CL^{pro}$): An *in silico* screening of alkaloids and terpenoids from African medicinal plants. *Journal of Biomolecular Structure and Dynamics*. https://doi.org/10.1080/07391102.2020.1764868

Harder, E., Damm, W., Maple, J., Wu, C., Reboul, M., Xiang, J. Y., Wang, L., Lupyan, D., Dahlgren, M. K., Knight, J. L., Kaus, J. W., Cerutti, D. S., Krilov, G., Jorgensen, W. L., Abel, R., & Friesner, R. A. (2016). OPLS3: A force field providing broad coverage of drug-like small molecules and proteins. *Journal of Chemical Theory and Computation*, *12*(1), 281–296. https://doi.org/10.1021/acs.jctc.5b00864

Hasan, A., Paray, B. A., Hussain, A., Qadir, F. A., Attar, F., Aziz, F. M., Sharifi, M., Derakhshankhah, H., Rasti, B., Mehrabi, M., Shahpasand, K., Saboury, A. A., & Falahati, M. (2020). A review on the cleavage priming of the spike protein on coronavirus by angiotensin-converting enzyme-2 and furin. *Journal of Biomolecular Structure and Dynamics*. https://doi.org/10.1080/07391102.2020.1754293

Hess, B., Bekker, H., Berendsen, H. J., & Fraaije, J. G. (1997). LINCS: A linear constraint solver for molecular simulations. *Journal of Computational Chemistry*, *18*(12), 1463–1472. https://doi.org/10.1002/(SICI)1096-987X(199709)18:12<1463::AID-JCC4>3.0.CO;2-H

Hilgenfeld, R. (2014). From SARS to MERS: Crystallographic studies on coronaviral proteases enable antiviral drug design. *The FEBS Journal*, *281*(18), 4085–4096. https://doi.org/10.1111/febs.12936

Huang, C., Wang, Y., Li, X., Ren, L., Zhao, J., Hu, Y., Zhang, L., Fan, G., Xu, J., Gu, X., Cheng, Z., Yu, T., Xia, J., Wei, Y., Wu, W., Xie, X., Yin, W., Li, H., Liu, M., … Cao, B. (2020). Clinical features of patientsinfected with 2019 novel coronavirus in Wuhan, China. *The* Lancet), *395*(10223), 497–506. https://doi.org/10.1016/S0140-6736(20)30183-5

Huang, C., Wei, P., Fan, K., Liu, Y., & Lai, L. (2004). 3C-like proteinase from SARS coronavirus catalyzes substrate hydrolysis by a general base mechanism. *Biochemistry*, *43*(15), 4568–4574. https://doi.org/10.1021/bi036022q

Islam, R., Parves, M. R., Paul, A. S., Uddin, N., Rahman, M. S., Mamun, A. A., Hossain, M. N., Ali, M. A., & Halim, M. A. (2020). A molecular modeling approach to identify effective antiviral phytochemicals against the main protease of SARS-CoV-2. *Journal of Biomolecular Structure and Dynamics*. https://doi.org/10.1080/07391102.2020.1761883

Joshi, R. S., Jagdale, S. S., Bansode, S. B., Shankar, S. S., Tellis, M. B., Pandya, V. K., Chugh, A., Giri, A. P., & Kulkarni, M. J. (2020). Discovery of potential multi-target-directed ligands by targeting host-specific SARS-CoV-2 structurally conserved main protease. *Journal of Biomolecular Structure and Dynamics*. https://doi.org/10.1080/07391102.2020.1760137

Kawata, M., & Nagashima, U. (2001). Particle mesh Ewald method for three-dimensional systems with two-dimensional periodicity. *Chemical Physics Letters*, *340*(1–2), 165–172. https://doi.org/10.1016/S0009-2614(01)00393-1

Khan, R. J., Jha, R. K., Amera, G. M., Jain, M., Singh, E., Pathak, A., Singh, R. P., Muthukumaran, J., & Singh, A. K. (2020). Targeting SARS-CoV-2: A systematic drug repurposing approach to identify promising inhibitors against 3C-like proteinase and 2′-O-ribose methyltransferase. *Journal of Biomolecular Structure and Dynamics*. https://doi.org/10.1080/07391102.2020.1753577

Khan, S. A., Zia, K., Ashraf, S., Uddin, R., & Ul-Haq, Z. (2020). Identification of chymotrypsin-like protease inhibitors of SARS-CoV-2 *via* integrated computational approach. *Journal of Biomolecular Structure and Dynamics*. https://doi.org/10.1080/07391102.2020.1751298

Kollman, P. A., Massova, I., Reyes, C., Kuhn, B., Huo, S., Chong, L., Lee, M., Lee, T., Duan, Y., Wang, W., Donini, O., Cieplak, P., Srinivasan, J., Case, D. A., & Cheatham, T. E. (2000). Calculating structures and free energies of complex molecules: combining molecular mechanics and continuum models. *Accounts of Chemical Research*, *33*(12), 889–897. https://doi.org/10.1021/ar000033j

Kumar, D., Kumari, k., Jayaraj, A., Kumar, V., Kumar, R. V., Dass, S. K., Chandra, R., & Singh, P. (2020). Understanding the binding affinity of noscapines with protease of SARS-CoV-2 for COVID-19 using MD simulations at different temperatures. *Journal of Biomolecular Structure and Dynamics*. https://doi.org/10.1080/07391102.2020.1752310

Kutzner, C., Van Der Spoel, D., Fechner, M., Lindahl, E., Schmitt, U. W., De Groot, B. L., & Grubmüller, H. (2007). Speeding up parallel GROMACS on high-latency networks. *Journal of Computational Chemistry*, *28*(12), 2075–2084. https://doi.org/10.1002/jcc.20703

Lai, C. C., Shih, T. P., Ko, W. C., Tang, H. J., & Hsueh, P. R. (2020). Severe acute respiratory syndrome coronavirus 2 (SARS-CoV-2) and coronavirus disease-2019 (COVID-19): The epidemic and the challenges. *International Journal of Antimicrobial Agents*, *55*(3), 105924. https://doi.org/10.1016/j.ijantimicag.2020.105924

Li, Y., & Xia, L. (2020). Coronavirus disease 2019 (COVID-19): Role of chest CT in diagnosis and management. *American Journal of Roentgenology*, *4*, 1–7.

Lobo-Galo, N., Terrazas-López, M., Martínez-Martínez, A., & Díaz-Sánchez, A. G. (2020). FDA-approved thiol-reacting drugs that potentially bind into the SARS-CoV-2 main protease, essential for viral replication. *Journal of Biomolecular Structure and Dynamics*. https://doi.org/10.1080/07391102.2020.1764393

Miyamoto, S., & Kollman, P. A. (1992). Settle: An analytical version of the SHAKE and RATTLE algorithm for rigid water models. *Journal of Computational Chemistry*, *13*(8), 952–962. https://doi.org/10.1002/jcc.540130805

Muralidharan, N., Sakthivel, R., Velmurugan, D., & Gromiha, M. M. (2020). Computational studies of drug repurposing and synergism of lopinavir, oseltamivir and ritonavir binding with SARS-CoV-2 protease against COVID-19. *Journal of Biomolecular Structure and Dynamics*. https://doi.org/10.1080/07391102.2020.1752802

Pant, S., Singh, M., Ravichandiran, V., Murty, U. S. N., & Srivastava, H. K. (2020). Peptide-like and small-molecule inhibitors against Covid-19. *Journal of Biomolecular Structure and Dynamics*. https://doi.org/10.1080/07391102.2020.1757510

Parrinello, M., & Rahman, A. (1981). Polymorphic transitions in single crystals: A new molecular dynamics method. *Journal of Applied Physics*, *52*(12), 7182–7190. https://doi.org/10.1063/1.328693

Sarma, P., Sekhar, N., Prajapat, M., Avti, P., Kaur, H., Kumar, S., Singh, S., Kumar, H., Prakash, A., Dhibar, D. P., & Medhi, B. (2020). In-silico homology assisted identification of inhibitor of RNA binding against 2019-nCoV N-protein (N terminal domain). *Journal of Biomolecular Structure and Dynamics*. https://doi.org/10.1080/07391102.2020.1753580

Sastry, G. M., Adzhigirey, M., Day, T., Annabhimoju, R., & Sherman, W. (2013). Protein and ligand preparation: Parameters, protocols, and influence on virtual screening enrichments. *Journal of Computer-Aided Molecular Design*, *27*(3), 221–234. https://doi.org/10.1007/s10822-013-9644-8

Schrödinger. (2017). *Schrödinger release 2017-1: LigPrep*. Schrödinger, LLC.

Schrödinger. (2017). *Schrödinger release 2017-1: Maestro*. Schrödinger, LLC.

Sinha, S. K., Shakya, A., Prasad, S. K., Singh, S., Gurav, N. S., Prasad, R. S., & Gurav, S. S. (2020). An *in-silico* evaluation of different Saikosaponins for their potency against SARS-CoV-2 using NSP15 and fusion spike glycoprotein as targets. *Journal of Biomolecular Structure and Dynamics*. https://doi.org/10.1080/07391102.2020.1762741

Specs Database. (1987). www.specs.net

Sterling, T., & Irwin, J. J. (2015). ZINC 15 – ligand discovery for everyone. *Journal of Chemical Information and Modeling*, *55*(11), 2324–2337. https://doi.org/10.1021/acs.jcim.5b00559

Wahedi, H. M., Ahmad, S., & Abbasi, S. W. (2020). Stilbene-based natural compounds as promising drug candidates against COVID-19. *Journal of Biomolecular Structure and Dynamics*. https://doi.org/10.1080/07391102.2020.1762743

Wang, C., Horby, P. W., Hayden, F. G., & Gao, G. F. (2020). A novel coronavirus outbreak of globalhealth concern. *The* Lancet, *395*(10223), 470–473. https://doi.org/10.1016/S0140-6736(20)30185-9

Xue, H., Li, J., Xie, H., & Wang, Y. (2018). Review of drug repositioning approaches and resources. *International Journal of Biological Sciences*, *14*(10), 1232–1244. https://doi.org/10.7150/ijbs.24612

Yang, H., Yang, M., Ding, Y., Liu, Y., Lou, Z., Zhou, Z., Sun, L., Mo, L., Ye, S., Pang, H., Gao, G. F., Anand, K., Bartlam, M., Hilgenfeld, R., & Rao, Z. (2003). The crystal structures of severeacute respiratory syndrome virus main protease and its complex with an inhibitor. *Proceedings* of the National Academy of Sciences, *100*(23), 13190–13195. https://doi.org/10.1073/pnas.1835675100

Zhang, L., Lin, D., Sun, X., Curth, U., Drosten, C., Sauerhering, L., Becker, S., Rox, K., & Hilgenfeld, R. (2020). Crystal structure of SARS-CoV-2 main protease provides a basis for design of improved α-ketoamide inhibitors. *Science*, *368*(6489), 409–412. https://doi.org/10.1126/science.abb3405